JOURNAL OF INTERFERON & CYTOKINE RESEARCH
Volume 39, Number 6, 2019

DOI: 10.1089/jir.2018.0163

DHX15 Is a Coreceptor for RLR Signaling That Promotes Antiviral Defense Against RNA Virus Infection

Sowmya Pattabhi,[1,2,*] Megan L. Knoll,[2,3] Michael Gale, Jr.,[1–3] and Yueh-Ming Loo[2,3]

RNA helicases play an important role in the response to microbial infection. Retinoic acid inducible gene-I (RIG-I) and members of the RIG-I-like receptor (RLR) family of helicases function as cytoplasmic pattern recognition receptors (PRRs) whose actions are essential for recognition of RNA viruses. RIG-I association with pathogen-associated molecular patterns (PAMPs) within viral RNA leads to its activation and signaling via the mitochondrial antiviral signaling (MAVS) adapter protein. This interaction mediates downstream signaling events that drive the innate immune response to virus infection. Here we identify the DEAH-box RNA helicase DHX15 as a RLR binding partner and signaling cofactor. In human cells, DHX15 is required for virus-induced RLR signaling of innate immune gene expression. Knockdown of DHX15 increased susceptibility to infection by RNA viruses of diverse genera, including Paramyxoviridae, Rhabdoviridae, and Picornaviridae. DHX15 associates with RIG-I caspase activation and recruitment domains (CARDs) through its amino terminus, in which the complex is recruited to MAVS on virus infection. Importantly, although DHX15 cannot substitute for RIG-I in innate immune signaling, DHX15 selectively binds PAMP RNA to promote RIG-I ATP hydrolysis and signaling activation in response to viral RNA. Our results define DHX15 as a coreceptor required for RLR innate immune responses to control RNA virus infection.

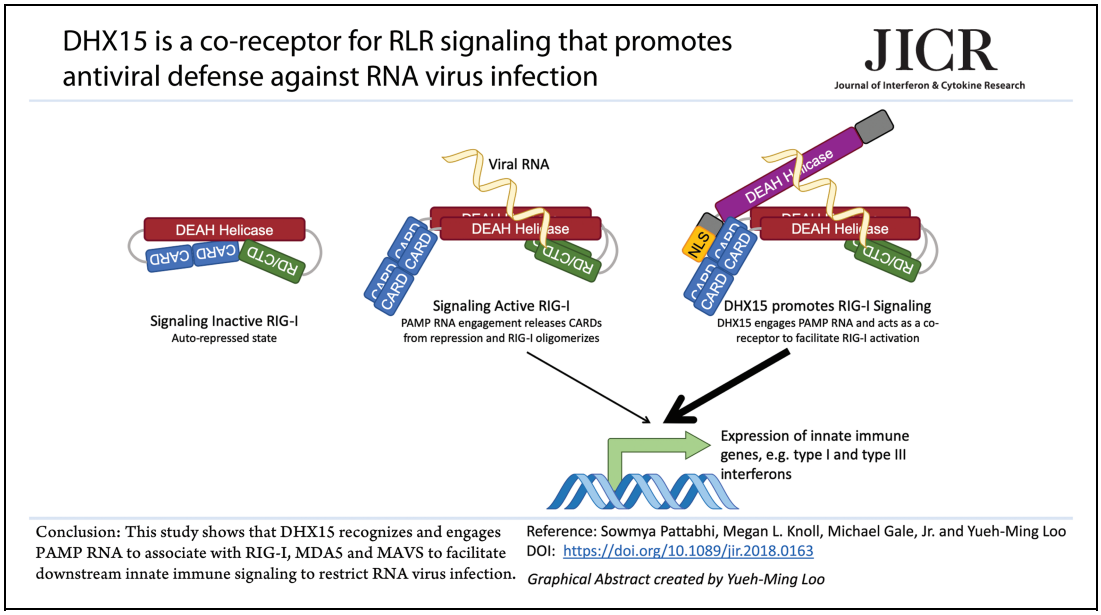

Color images are available online.

Keywords: RIG-I, MDA5, DHX15, innate immunity, RNA virus, MAVS

This work uses data collected within the framework of the PhD thesis ''Exploring RIG-I like receptor signaling: Regulation by DHX15 and RIGing the pathway for broad spectrum antiviral immunity'' of Sowmya Pattabhi in 2015 at the University of Washington.

Departments of [1]Global Health and [3]Immunology, University of Washington, Seattle, Washington.
[2]Department of Immunology, Center for Innate Immunity and Immune Disease, University of Washington, Seattle, Washington.
**Current affiliation:* Seattle Children's Research Institute, Seattle, Washington.

Introduction

THE CELL-INTRINSIC INNATE immune response is our first line of defense against virus infection and is initiated when cellular pattern recognition receptors (PRRs) recognize and bind to pathogen-associated molecular patterns (PAMPs) presented within products of virus infection, including viral RNA. The PAMP-PRR interaction triggers signaling cascades that culminate in the expression of host innate immune defense genes that serve to restrict virus replication and spread. Interferons (IFNs) and cytokines that are secreted as a consequence of this signaling cascade amplify the host response through receptor-mediated signaling that induces the expression of interferon-stimulated genes (ISG) and cytokine response genes whose products mediate antiviral actions and serve to program the adaptive immune response to infection (Brubaker and others 2015).

The retinoic acid inducible gene-I (RIG-I)-like receptors (RLRs), including RIG-I, melanoma differentiation-associated protein 5 (MDA5), and laboratory of genetics and physiology 2 (LGP2), are a family of cytoplasmic DExD/H RNA helicases that mediate the detection of RNA viruses (Kato and others 2017; Chow and others 2018). While each encodes RNA helicase domains of the SF2 helicase superfamily, they have inherent ATPase activity that governs their signaling actions (Luo and others 2013; Fitzgerald and others 2017). Moreover, RIG-I and MDA5 contain tandem N-terminal caspase activation and recruitment domains (CARDs) that impart downstream signaling interaction with the mitochondrial antiviral signaling (MAVS) adaptor protein, whereas LGP2 lacks the CARDs and is thought to be a regulator or cofactor of the other RLRs (Yoneyama and others 2005; Deddouche and others 2014).

RLR signaling is tightly coordinated by expression level, PAMP binding, and induction of ATPase activity, and by autoregulatory conformation state changes conferred by a repressor domain (RD) present in the carboxy terminus (Saito and others 2007). In resting cells, RLRs are maintained at low expression levels and intramolecular interactions between the RD with the CARDs and helicase domain sequester the CARDs from signaling to hold the RLR in a signaling-inactive conformation. However, expression is rapidly increased after virus infection or IFNs. In the case of RIG-I, engagement of viral RNA harboring a 5′-triphosphate moiety along with double-stranded RNA (dsRNA) structure or polyuridine-rich single-stranded RNA (ssRNA) sequence interspersed with cytosine bases (polyU/UC) (Hornung and others 2006; Saito and Gale 2008; Schnell and others 2012) induces it to hydrolyze ATP.

The CARDs are released from autorepression by the RD to assume a signaling-on conformation that permits its recruitment and binding to MAVS on mitochondria-associated membranes (MAM) (Gack and others 2007; Michallet and others 2008; Horner and others 2011; Liu and others 2012). RLR association with MAVS activates downstream transcription factors, including interferon regulatory factor 3 (IRF3) and NF-κB, to drive innate immune gene expression and response (Imaizumi and others 2007, 2008, 2010; Kitamura and others 2007; Loo and others 2008; Tsugawa and others 2008). These processes of RIG-I activation and signaling are regulated, in part, through cofactor interactions that govern its activation and interaction with MAVS (Matsumiya and others 2009; Loo and Gale 2011; Liu and others 2012; Gack 2014).

Importantly, there is increasing evidence supporting the involvement of non-RLR DExD/H helicases in regulating innate immune signaling pathways in controlling viral infection. For example DDX21, DHX36, DDX1, and DHX9 have been shown to be important for the control of Toll-like receptor signaling in response to virus infection (Kim and others 2010; Zhang and others 2011a), while DDX41 and DHX33 have been identified as helicases that signal through stimulator of interferon genes (STING) to establish an innate immune program against DNA viruses (Zhang and others 2011b; Mitoma and others 2013). DHX33 is further shown to regulate inflammatory signaling through the NLRP3 inflammasome (Mitoma and others 2013) and has been implicated as a PRR that signals through MAVS to induce dendritic cell activation in response to dsRNA such as synthetic polyinosinic-polycytidylic acid [poly(I:C)] and reovirus RNA (Liu and others 2014). In addition, DDX3, DHX9, DHX29, DHX36, DDX60, and DDX24 have been shown to regulate the RLR pathway (Oshiumi and others 2010; Miyashita and others 2011; Zhang and others 2011c; Ma and others 2013; Sugimoto and others 2014; Yoo and others 2014). These observations indicate that non-RLR DExD/H box helicases can serve as cofactors in innate immune and inflammatory signaling programs and function as RLR cofactors.

A wide variety of proteins have been identified as RLR binding and signaling cofactors, revealing that cofactor activity is essential for RLR signaling that controls innate immunity and the response to virus infection. We used a proteomic approach to identify and define RIG-I binding partners (Liu and others 2012), and we now report the identification of DHX15, a DExD/H box helicase, as an RLR-binding partner and signaling cofactor.

DHX15 was previously identified as a pre-messenger RNA (mRNA) processing factor involved in the disassembly of spliceosomes and the debranching or turnover of excised introns (Deckert and others 2006; Wen and others 2008; Yoshimoto and others 2009). In intestinal epithelial cells, DHX15 has been shown to function in conjunction with NLRP6 to sense viral RNA to signal MAVS-dependent induction of type I and type III IFNs (Wang and others 2015). Other studies further implicate DHX15 as an activator of mitogen-activated protein kinase (MAPK) signaling and required for IFN-β, interleukin-6 (IL-6), and TNFα production in response to poly(I:C) RNA transfection and RNA virus infection in dendritic cells (Lu and others 2014; Mosallanejad and others 2014). However, it is unclear how DHX15 functions to signal innate immune defenses in the context of the RLRs.

Our studies reveal that cells lacking DHX15 expression exhibit a defect in innate immune responses to RNA virus infection and are correspondingly more susceptible to virus replication. DHX15 can selectively bind to PAMP RNA, and virus infection promotes DHX15 interactions with both RIG-I and MAVS. DHX15 can additionally interact with MDA5. Although it cannot substitute for RIG-I to signal innate immune responses, the presence of DHX15 promotes greater RIG-I hydrolysis of ATP in response to PAMP RNA. Importantly, ectopic expression of DHX15 facilitated greater innate immune signaling in response to RNA virus infection. The data strongly suggest that DHX15 may function to lower the threshold for RIG-I signaling activation. Thus, DHX15 is a coreceptor for viral RNA required for RLR signaling and innate antiviral immunity to control RNA virus infection.

Materials and Methods

Cell lines

Huh7 (human hepatocyte) and HEK293 (human embryonic kidney epithelial) cell lines were cultured in Dulbecco's modified Eagle's media (Cellgro) supplemented with 10% fetal bovine serum (FBS; HyClone), L-glutamine, sodium pyruvate, and nonessential amino acids. The THP-1 (human monocytic) cell line was cultured in complete RPMI 1640 media (Invitrogen) supplemented with 10% heat-inactivated FBS, L-glutamine, sodium pyruvate, and nonessential amino acids. THP-1 cells were differentiated into macrophage-like cells in complete RPMI 1640 supplemented with 40 nM phorbol myristate acetate (PMA).

Viruses

Sendai virus (SeV, Cantell strain) stocks were purchased from Charles River Laboratories. Encephalomyocarditis virus (EMCV) and vesicular stomatitis virus (VSV) have been described before and were titered by standard plaque assay on Vero cells (Yoneyama and others 2004). Cells were inoculated with virus in serum-free media at a multiplicity of infection (MOI) of 0.01 for EMCV or VSV and a concentration of SeV that ranged between 50 and 200 hemagglutination units (HAU)/mL. Lentivirus particles for creating knockdown cells were purchased from the Sigma-Aldrich MISSION short hairpin RNA (shRNA) collection and express the following shRNA sequences: DHX15 (CCGGGTTGG TTCGATAATGGCCTTTCTCGAGAAAGGCCATTATCG AACCAACTTTTT, catalog No. TRCN0000000006), MAVS (CCGGCAAGTTGCCAACTAGCTCAAACTCGAGTTT GAGCTAGTTGGCAACTTGTTTTTTG, catalog No. TRCN0000148945), RIG-I (CCGGAGCACTTGTGGACG CTTTAAACTCGAGTTTAAAGCGTCCACAAGTGCTTTT TTG, catalog No. TRCN0000230212), and the nontargeting shRNA control [nontargeting vector (NTV); CCGGCAA CAAGATGAAGAGCACCAACTCGAGTTGGTGCTCTTCA TCTTGTTGTTTTT, catalog No. SHC002].

Plasmids

RIG-I, MDA5, MAVS, TBK1, IKKε, and IRF3 expression constructs have been described (Sumpter and others 2005; Loo and others 2006; Saito and others 2007). MAVS mutants lacking the N-terminal CARD (ΔCARD), the C-terminal transmembrane domain (ΔTM), or both (ΔTMΔCARD) were created by using the QuikChange site-directed mutagenesis kit (Stratagene). DHX15 complementary DNA (cDNA; RC205914; OriGene) was cloned into vectors pEFTak and pCMV6 (PS100012 or PS100014; OriGene) for expression as N-terminally Flag- or myc-tagged proteins. DHX15 truncation and point mutants were created using the QuikChange II XL lightning site-directed mutagenesis kit (Agilent Technologies). Primer sequences are available on request. Promoter luciferase reporter plasmids pIFN-β-luc, pIFIT1-luc, and pCMV-*Renilla*-luc have been previously reported (Foy and others 2003; Li and others 2005).

Antibodies

The following primary antibodies were used for immunoblot detection: rabbit anti-RIG-I (raised in rabbit against an RIG-I CARD peptide sequence) (Loo and others 2008), rabbit anti-MAVS (AT107; Enzo Life Sciences), rabbit anti-MDA5 (AT113; Enzo Life Sciences), rabbit anti-DHX15 (AB70454; Abcam), rabbit anti-myc (AB9106; Abcam), and HRP-conjugated mouse anti-Flag (A8592; Sigma). Monoclonal antibodies used for immunoprecipitation include the following: mouse anti-RIG-I (Alme-1; AdipoGen), mouse anti-MAVS IgG2b (Enzo Life Sciences), mouse anti-DDX15 IgG2a (E-6; Santa Cruz Biotechnology), mouse anti-Flag M2 IgG1 (F3165; Sigma), and mouse anti-c-myc (9E10; Santa Cruz Biotechnology). HRP-conjugated secondary antibodies were obtained from Jackson ImmunoResearch.

RNA

The synthetic dsRNA poly(I:C) was purchased from InvivoGen. The hepatitis C virus (HCV) xRNA and polyU/UC RNA were *in vitro* transcribed from synthetic DNA oligonucleotide templates (Integrated DNA Technologies) using the T7 MEGAshortscript kit (Ambion) as previously described (Saito and others 2008; Schnell and others 2012). xRNA and polyU/UC RNA were labeled using the Thermo Scientific Pierce RNA 3′ End Biotinylation Kit.

Real-time polymerase chain reaction

Cells were collected in RLT buffer at the indicated times and total cellular RNA purified using the RNeasy Mini Kit (Qiagen). Total cDNA was synthesized from purified RNA using a combination of random oligo and oligo (dT) primers and the iScript cDNA synthesis kit (Bio-Rad Laboratories). Host and viral RNA levels were determined using SYBR Green (Applied Biosystems) and the 7300 real-time polymerase chain reaction (RT-PCR) system (Applied Biosystems). The relative expression level of host and viral genes was calculated as fold change over mock-infected controls, normalized to *GAPDH* using the ΔΔCT method. RT-PCR primer sequences are listed in Supplementary Table S1 with the exception of the *IL-6* primers, which were obtained from SA Biosciences.

Measuring infectious virus particles

Huh7 and HEK293 cells were infected at an MOI of 0.01 with EMCV for 18 h or VSV for 12 h. Cell culture supernatant was collected at the indicated time points postinfection. Infectious viral particles in the supernatant were measured by standard plaque assay using serial dilutions and with agar overlay on Vero cells. Plaques were stained with neutral red and counted 24 h after infection.

Immunoprecipitation and immunoblot analyses

Cell lysates were collected in RIPA buffer [50 mM Tris-HCl pH 7.5, 150 mM NaCl, 5 mM EDTA, 1% (v/v) NP-40, 0.5% (v/v) sodium deoxycholate, 0.1% (v/v) sodium dodecyl sulfate (SDS)] supplemented with a mammalian protease inhibitor cocktail (Sigma-Aldrich), phosphatase inhibitor cocktail, and okadaic acid (Calbiochem) and clarified by centrifugation at 15,000*g* for 10 min at 4°C. Cell lysates were quantified by BCA (Thermo Scientific) and a standard amount of protein taken across samples for each immunoprecipitation. Immunoprecipitations were performed using the antibody of choice and protein G Dynabeads (GE Life Sciences) in RIPA buffer. Beads were washed 3–5 times

with RIPA buffer before the proteins were eluted in sodium dodecyl sulfate/polyacrylamide gel electrophoresis (SDS-PAGE) sample buffer. Proteins were detected by immunoblot analyses and visualized using the ECL prime substrate (GE Life Sciences).

Immunoprecipitation and mass spectrometry

Flag-tagged N-terminus of RIG-I (N-RIG) was overexpressed in HEK293 cells and immunoprecipitated with the anti-Flag M2 antibody. The proteins that were eluted were trypsin digested and run on a nano-high-performance liquid chromatography using a 5 cm Magic C18 Column (Michrom Bioresources, Auburn, CA) using a buffer system of (A) water +0.1% formate and (B) acetonitrile +0.1% formate (Avantor Performance Materials, Phillipsburg, NJ) in a 60-min gradient from 98% A/2% B to 5% A/95% B. The peptides were separated and detected on a linear ion trap mass spectrometer (LTQ; Thermo Fisher Scientific) based on their mass to charge ratio and the peptide sequence determined. The predicted sequence was searched against human IPI v3.28 database using SEQUEST to identify and match sequences present in the database. The results of these searches were analyzed using PeptideProphet and ProteinProphet. Proteins that were identified with at least 2 unique peptides or more, with a probability score of 0.99–1, were identified as reliable hits (Liu and others 2012).

ATPase assay

The DHX15 recombinant protein was expressed in *Escherichia coli* using expression vector E3 and purified from inclusion bodies to ~95% purity as estimated by densitometric analysis of the Coomassie blue-stained SDS-PAGE gel (GenScript). The RIG-I recombinant protein was a gift from Joe Marcotrigiano and was previously described (Saito and others 2008; Schnell and others 2012). ATPase assays were performed as previously described (Schnell and others 2012). Briefly, various amounts of RNA (0–1 pmol) were mixed with 5 pmol purified DHX15 or RIG-I protein in a total of 25 μL ATPase reaction buffer (20 mM Tris-HCl pH 8.0, 1.5 mM $MgCl_2$, 1.5 mM DTT). Reactions were incubated at 37°C for 15 min, ATP (Sigma) was added to a final concentration of 1 mM, and the reactions incubated at 37°C for 15 min. Absorbance of each sample in BIOMOL Green reagent (Enzo Life Sciences) was measured at OD_{630nm} in a microplate format and the free phosphate concentration calculated based on the standard curve.

Filter binding assay

Purified recombinant DHX15 was mixed with biotinylated polyU/UC RNA or biotinylated xRNA in reaction buffer consisting of 20 mM Tris-HCl pH 8.0, 1.5 mM $MgCl_2$, and 1.5 mM DTT at 37°C for 15 min and spotted onto nitrocellulose membranes (Millipore) using the Bio-dot SF microfiltration apparatus (Bio-Rad Laboratories) according to the manufacturer's instructions. The membranes were blocked in a blocking buffer (LI-COR). DHX15 was detected using a rabbit anti-DHX15 (Abcam) antibody and IRDye 680RD donkey anti-rabbit IgG (LI-COR). Protein-bound RNA was detected using IRDye 800CW streptavidin (LI-COR). Imaging was performed using the Odyssey CLx imager and analyzed using the Image Studio software (LI-COR).

RNA pulldown assay

Recombinant DHX15 or RIG-I proteins were generated by *in vitro* transcription and translation reactions using the TNT Quick Coupled Transcription/Translation system (Promega). xRNA, polyU/UC, and poly(I:C) RNA were 3′ end-labeled with biotin using T4 RNA ligase and immobilized on streptavidin M280 beads (Thermo Fisher) at a 10× saturation concentration in binding buffer (5 mM Tris-HCl pH 7.5, 0.5 mM EDTA, 1 M NaCl) supplemented with RNase inhibitors (Thermo Fisher). Excess unbound RNA was removed by repeated washing before the beads were incubated with TNT lysates diluted in RIPA buffer. Following successive rounds of washing, RNA-bound protein was assessed by immunoblot analysis. A fraction of the TNT lysate was directly assessed by immunoblot analysis as input.

Promoter luciferase assay

Procedures were described previously (Loo and others 2008). Briefly, cells were cotransfected with *Renilla* luciferase and either pIFN-β-luciferase or pIFIT1-luciferase constructs, and simultaneously transfected with the appropriate constructs for ectopic expression of DHX15, RIG-I, or other innate immune components, if any. Cells were either treated with 100 IU/mL IFN-β or infected with virus or mock-infected 18 h after transfection. At the indicated times, cell extracts were collected and analyzed for dual luciferase activity (Promega).

Statistical analyses

All statistical analyses were performed using the GraphPad Prism 7.04 software, using 2-way analysis of variance (ANOVA) with Bonferroni post-tests, 1-way ANOVA, or *t*-test as appropriate. The interaction between cell types (DHX15, RIG-I, MAVS, NTV stable knockdown cells) at different time points or MOI was compared. The RNA binding and ATPase analyses were evaluated by linear regression analysis. GraphPad Prism version 7.04 was used to compare slopes of 2 or more regression lines to test whether the slopes were significantly different. *P* values are directly reported where possible or summarized as follows: ns for $P > 0.05$, * for $P \leq 0.05$, ** for $P \leq 0.01$, *** for $P \leq 0.001$, and **** for $P \leq 0.0001$.

Results

DHX15 is an RIG-I binding protein and component of the RLR signaling complex required for the control of RNA virus infections

A combination of immunoprecipitation and proteomic approach was used to identify signaling cofactors that associate with signaling-active RIG-I. For this purpose, a Flag-tagged RIG-I construct consisting entirely of the 2 N-terminal tandem CARDs (N-RIG), mediating constitutive signaling through MAVS, was ectopically expressed in HEK293 cells. Proteins that associate with the activated RIG-I-MAVS complex were recovered through Flag-N-RIG immunoprecipitation and identified by mass spectrometry (Liu and others

2012). This proteomic approach identified a total of 244 cellular factors with a probability score of 0.99 or greater. The score is based on the number of unique peptides identified and the probability that the peptides from the sample reliably match those in the protein database (Perkins and others 1999).

Elimination of factors that were present in control immunoprecipitations (using a construct expressing 2× Flag alone) then revealed potential RIG-I cofactors. Among the resulting list of proteins were several proteins known to associate with and regulate RLR signaling, including DDX3, ISG15, DDX58, and 14-3-3ε (Liu and others 2012). Importantly, included among these proteins that associate with the RIG-I CARDs is DHX15, which was identified from 3 unique peptide sequences with a probability score of 1.

We performed coimmunoprecipitation studies to define DHX15 interaction with RIG-I. When coexpressed in human hepatoma (Huh7) cells, Myc-tagged DHX15 forms a stable complex with Flag-RIG-I, indicating that DHX15 can interact with an overexpressed full-length RIG-I protein (Fig. 1A). To determine if DHX15 is involved in RIG-I signaling, we assessed whether suppression of DHX15 expression in human cells had an impact on RIG-I-dependent signaling responses. We created a stable Huh7 cell line with shRNA knockdown of DHX15 expression. For control, we created a Huh7 cell line that stably expressed a nontargeting shRNA (NTV) that will similarly activate the RNA interference (RNAi) pathway but is not known to target any human or mouse genes.

Comparison of RNA expression in each cell line confirmed a 60% knockdown of DHX15 mRNA expression compared with control NTV cells (Fig. 1B). Using similar methods, we also created Huh7 cell lines with 80% knockdown of MAVS or ~60% knockdown of RIG-I compared with NTV cells. Infection of the NTV control cells with SeV resulted in robust induction of the IFIT1 promoter compared with mock-infected cells in luciferase reporter assays, but cells with knockdown of DHX15, MAVS, or RIG-I showed little or no induction of the IFN-β promoter (Fig. 1C). Reconstitution of DHX15 expression in knockdown cells with a nontargeted DHX15 construct restores SeV-induced signaling to the *IFN-β* promoter (Fig. 1D). By Western blot, we confirm expression of Flag-DHX15 in the knockdown cells (Fig. 1E). In Huh7 cells, SeV-induction of innate immune responses is dependent on RIG-I and MAVS with subsequent amplification by type I and type III IFNs (Diamond and Farzan 2013).

In comparison with NTV controls, Huh7 cells with knockdown of DHX15 were similarly defective as cells with knockdown of MAVS (Fig. 1F) for expression of many innate immune genes, including *IFIT1*, *IFIT2*, *DDX58*, and *MX1*. In macrophage-like THP-1 cells, we also observed a defect for *IFN-β*, *IL-1b*, *TNFα*, and *IL-6* expression in response to SeV infection with DHX15 knockdown compared with NTV control (Fig. 1G). Correspondingly, cells with DHX15 knockdown exhibit a 0.5 log increase in SeV RNA (Fig. 1H) and an ~1.0 log increase in VSV titer (Fig. 1I). Thus, cells lacking DHX15 expression exhibit a greater susceptibility for replication of 2 viruses from distinct families that signal innate immune responses in an RIG-I-dependent manner (Kato and others 2005, 2006; Loo and others 2008). Therefore, DHX15 is an RIG-I binding protein that is required for effective RIG-I-mediated innate immune signaling and control of RNA virus infection.

To further define the role of DHX15 in innate immune signaling, we assessed whether DHX15 is required for cells to respond to IFN. Control NTV cells and Huh7 cells with DHX15 knockdown were exposed to media supplemented with or without exogenous IFN-β and evaluated for IFIT1

FIG. 1. DHX15 is an RIG-I-interacting protein that signals innate immune responses and required for antiviral immunity against RNA viruses. **(A)** HEK293 cells were cotransfected with FLAG-RIG-I and either a control Myc-vector or a plasmid expressing Myc-DHX15. Myc-DHX15 was immunoprecipitated and coprecipitating FLAG-RIG-I was analyzed by immunoblot analysis. Total cell lysate was analyzed directly by SDS-PAGE immunoblot as input. **(B)** The relative gene expression levels (%) of the genes, *DHX15*, *RIG-I*, and *MAVS*, in Huh 7 knockdown cells that stably express shRNA to *DHX15*, *RIG-I*, *MAVS*, or a control sequence not found in human or mouse cells (NTV) as measured by RT-PCR analysis. **(C)** Huh7 knockdown cells were cotransfected with *ISG56/IFIT1* promoter-driven firefly luciferase reporter plasmid and a CMV promoter-driven *Renilla* luciferase reporter plasmid. Cells were mock-infected or infected with SeV for 24 h and then analyzed for dual luciferase activity. The results are expressed as average fold change in relative promoter activity of SeV-infected cells over mock-infected cells. **(D)** Huh7 knockdown cells were cotransfected with an *IFN-β* promoter-driven firefly luciferase reporter plasmid, a CMV promoter-driven *Renilla* luciferase reporter plasmid, and either a vector control plasmid or a plasmid that ectopically expressed either Flag-DHX15 or the Flag-DHX15 AAAA mutant. Cells were mock-infected or infected with SeV for 24 h and then analyzed for dual luciferase activity. The results are expressed as average fold change in relative promoter activity of SeV-infected cells over mock-infected cells. **(E)** Representative immunoblot showing expression of Flag-DHX15 and Flag-DHX15 AAAA relative to a tubulin loading control using cell lysates generated in parallel with **(D)**. **(F)** Huh7 or **(G)** PMA-differentiated THP-1 knockdown cells were mock-infected or infected with SeV. Total cellular RNA was collected at 0, 6, 12, 18, and 24 h postinfection and analyzed by RT-PCR for various innate immune, cytokine, and IFN genes, normalized to *GAPDH*. Graphs show average fold induction over mock-infected controls with error bars showing standard deviation. **(H)** Huh7 knockdown cells were mock-infected or infected with SeV and total cellular RNA collected at 0, 6, 12, 18, and 24 h postinfection and analyzed by RT-PCR for SeV genomic RNA against a standard. Results show average SeV RNA copy number from 3 independent experiments with error bars showing standard deviation. **(I)** Huh7 knockdown cells were mock-infected or infected with VSV at an MOI of 0.01 for 12 h. Infectious virus particle numbers in the cell culture supernatant were measured by plaque assay on Vero cells at 24 h postinfection. Results show average infectious virus particle numbers calculated per milliliter supernatant from 3 independent experiments. $*P \le 0.05$, $**P \le 0.01$, $***P \le 0.001$ and $****P \le 0.0001$. IFN, interferon; ISG, interferon-stimulated genes; MAVS, mitochondrial antiviral signaling; MOI, multiplicity of infection; NTV, nontargeting vector; PMA, phorbol myristate acetate; RIG-1, retinoic acid inducible gene-I; RT-PCR, real-time polymerase chain reaction; SDS-PAGE, sodium dodecyl sulfate/polyacrylamide gel electrophoresis; SeV, Sendai virus; shRNA, short hairpin RNA; VSV, vesicular stomatitis virus.

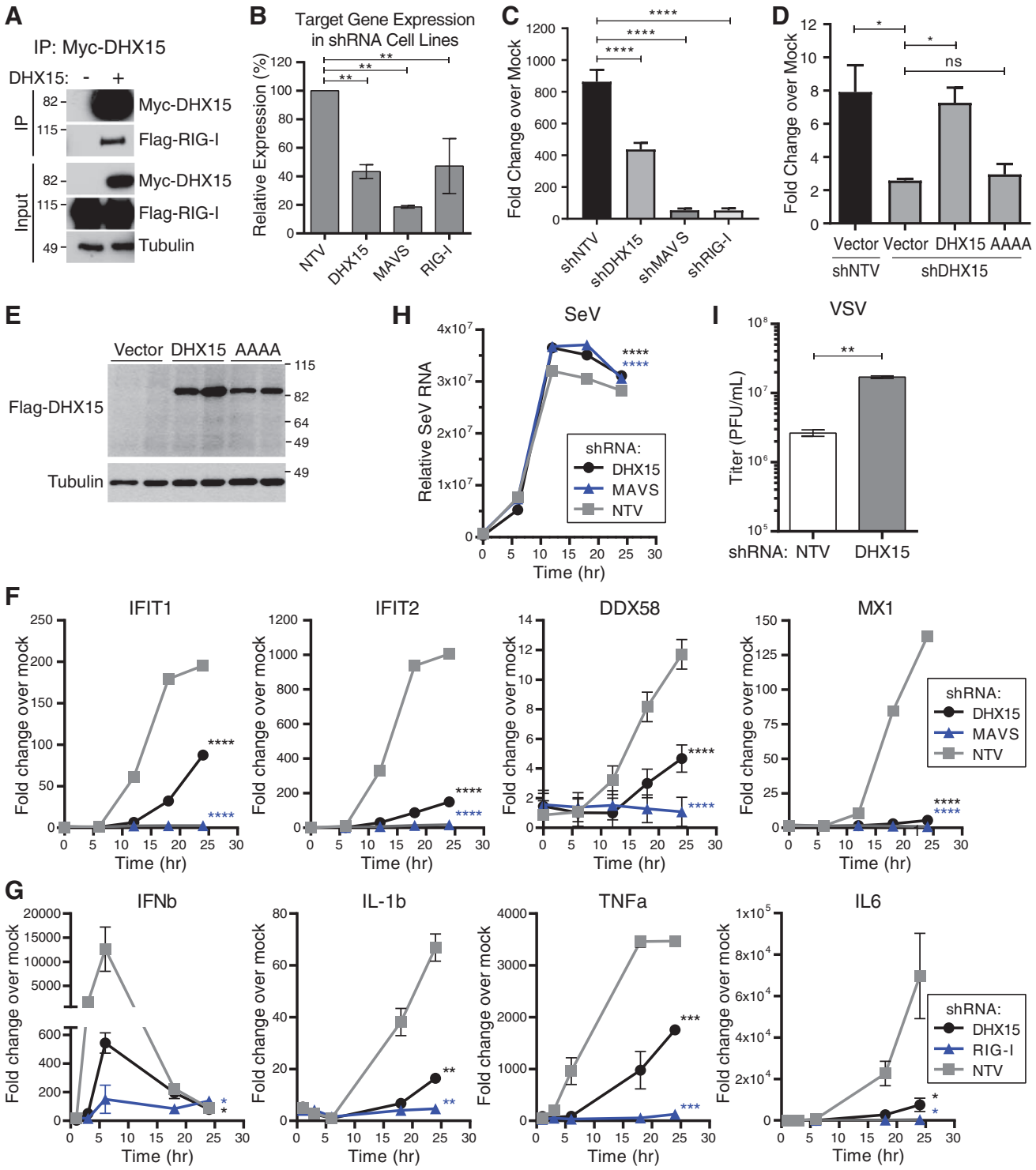

promoter activation. Cells lacking DHX15 expression retain the ability to induce IFIT1 promoter activation similar to NTV control cells (Fig. 2A). Furthermore, DHX15 is not itself an ISG as its expression remains constant in cells even after treatment with 100 IU/mL of IFN-β for up to 24 h (Fig. 2B). In contrast, IFIT1 mRNA can be observed to accumulate over time with IFN-β treatment. Taken together, our data indicate that DHX15 functions upstream of the type I IFN receptor within the context of innate immune signaling.

To define whether interactions between RIG-I and DHX15 are induced by virus infection, we performed immunoprecipitation studies of endogenous DHX15 and RIG-I from within Huh7 cells that were mock-infected or infected with SeV (Fig. 2C). We detected little DHX15 association with RIG-I in mock-infected cells in which RIG-I is maintained at low levels and in its signaling-off state (Sumpter and others 2005; Saito and others 2007; Chow and others 2018). In contrast, we found abundant

RIG-I in a stable complex with DHX15 after SenV infection, in which RIG-I is activated and its levels are increased, suggesting that the DHX15-RIG-I interaction is induced by virus infection and/or increased RIG-I levels to involve the signaling active form of RIG-I. Notably, we also detected the presence of MAVS within the virus-induced RIG-I-DHX15 complex. As RIG-I and MAVS associate when innate immune signaling is turned on, our data confirm the signaling-active state of RIG-I. The data further indicate that DHX15 can associate with the signaling-active RIG-I and MAVS complex during virus infection.

To define DHX15's role in the RLR-signaling pathway, we conducted epistasis experiments in DHX15 knockdown cells, in which we evaluated signaling that is induced by the overexpression of MAVS, the IRF3 kinases, TBK1 and IKKε, signaling-active mutants encoding tandem CARDs of RIG-I (N-RIG) or MDA5 (N-MDA5), or an IRF3 mutant that is constitutively active in signaling (IRF3-5D) (Lin and others 1999; Fitzgerald and others 2003; Yoneyama and others 2004; Sumpter and others 2005; Loo and others 2006). Expression of TBK1, IKKε, and IRF3-5D in DHX15-knockdown cells each restored signaling to the IFN-β promoter to levels observed in NTV control cells. In contrast, expression of N-RIG, N-MDA5, and MAVS did not (Fig. 2D) despite similar expression levels of each of these proteins in NTV and DHX15 knockdown cells. The data suggest that DHX15 regulates innate immune signaling actions at or above the level of MAVS, and further reveal a possible parallel role for DHX15 in the regulation of MDA5 signaling.

We performed immunoprecipitation studies to verify DHX15 associations with MDA5 and MAVS. As expected, Flag-DHX15 formed a complex with Myc-RIG-I, with the interaction enhanced by SeV infection (Fig. 2E). Flag-DHX15 also coprecipitated with Myc-MDA5 and Myc-MAVS but not with the Myc-vector control. DHX15 interaction with MDA5 and MAVS is not observed to be enhanced with SeV as in the case with RIG-I. However, as MDA5 and MAVS overexpression has been shown to be sufficient for initiation of innate immune signaling (Yoneyama and others 2004; Kawai and others 2005; Meylan and others 2005; Seth and others 2005; Xu and others 2005; Loo and others 2006; Errett and others 2013), these data are consistent with a hypothesis that DHX15 interacts favorably with an active RLR-MAVS complex.

Importantly, cells with DHX15 knockdown are defective for expression of IFN-β, IFNL2, IL-6, and numerous innate immune genes in response to the overexpression of NMDA5 (Fig. 2F), a construct that consists of the N-terminal tandem CARDs of MDA5 alone that potently activates MDA5-dependent innate immune signaling (Yoneyama and others 2005). Correspondingly, these cells exhibit greater susceptibility for EMCV replication (Fig. 2G). Since EMCV is a virus known to induce MDA5- but not RIG-I-dependent innate immune responses (Kato and others 2006), the data demonstrate that DHX15 is also important for MDA5 control of virus infection. Taken together, our data indicate that DHX15 is a cofactor required for RLR signaling to innate immunity during virus infection.

DHX15 interacts with the RIG-I CARDs

Focusing on the interactions between DHX15 and RIG-I, we performed coimmunoprecipitation studies with truncation mutants to define the protein domains that are important for the observed interactions. The RIG-I protein structure consists of N-terminus tandem CARDs that confer signaling action, a highly conserved helicase domain typical of DExD/H box helicases, and a C-terminus RD important for autoregulation (Fig. 3A) (Yoneyama and others 2004, 2005). Of the mutants tested, only the Flag-RIG-I aa 1–228

FIG. 2. DHX15 interacts with RIG-I, MDA5, and MAVS to initiate innate immune responses upstream of IFNAR signaling. **(A)** Huh7 knockdown cells were cotransfected with an ISG56/IFIT1 promoter-driven firefly and CMV promoter-driven *Renilla* luciferase reporter plasmids. Cells were mock-treated or treated with exogenous IFN-β in the media for 24 h and analyzed for dual luciferase activity. Results are expressed as relative luciferase activity. **(B)** Huh7 cells were treated with IFN-β (100 IU/mL). Cells were collected at 2, 12, or 24 h and the relative expression of the *ISG56/IFIT1* and *DHX15* genes was measured by RT-PCR, normalized to *GAPDH* and expressed as fold-induction over the mock-treated control. **(C)** HEK293 cells were mock-infected or infected with SeV for 7 h. Endogenous DHX15 was immunoprecipitated from cell lysates. DHX15 and coprecipitating proteins were eluted using SDS-PAGE sample buffer and analyzed by Western blot analysis. Total cell lysate was analyzed directly as input. **(D)** Huh7 knockdown cells (NTV control or DHX15 knockdown cells) were cotransfected with the *IFN-β* promoter-driven firefly luciferase reporter plasmid, a CMV promoter-driven *Renilla* luciferase reporter plasmid, and either a vector control plasmid or a plasmid that ectopically expressed constitutively active signaling factors of the RLR pathway: N-RIG, N-MDA5, MAVS, TBK-1, IKKε, and IRF3-5D. Lysates were collected 24 h after transfection and analyzed for dual luciferase reporter activity. The results are expressed as relative luciferase activity. Error bars show standard deviations. **(E)** HEK293 cells were cotransfected with FLAG-DHX15 along with an Myc-vector control or plasmids expressing Myc-RIG-I, Myc-MDA5, or Myc-MAVS. Cells were either mock-infected or infected with SeV for 24 h. Myc-tagged proteins were immunoprecipitated from cell lysates and analyzed by immunoblot for Myc-tag proteins and coprecipitating FLAG-DHX15 protein. Total cell lysate was analyzed directly by Western blot as input. **(F)** Huh7 knockdown cells were transfected with a vector control or a plasmid expressing NMDA5 (MDA5 CARDs alone) to turn on MDA5-specific innate immune signaling. Total RNA was collected 18 h post-transfection and analyzed by RT-PCR for expression of various IFN, cytokine, and innate immune genes. The graphs show average fold gene induction with NMDA5 overexpression relative to vector transfection controls. **(G)** Huh7 knockdown cells were mock-infected or infected with EMCV at an MOI of 0.01 for 18 h. Infectious virus particles in the cell culture supernatant were measured by plaque assay on Vero cells at 24 h postinfection. Results show average infectious virus particle numbers calculated per milliliter cell culture supernatant from 3 independent experiments. ns, $P > 0.05$; $*P \leq 0.05$, $**P \leq 0.01$, $***P \leq 0.001$ and $****P \leq 0.0001$. CARDs, caspase activation and recruitment domains; EMCV, encephalomyocarditis virus; IRF3, interferon regulatory factor 3; MDA5, melanoma differentiation-associated protein 5; RLR, RIG-I-like receptor.

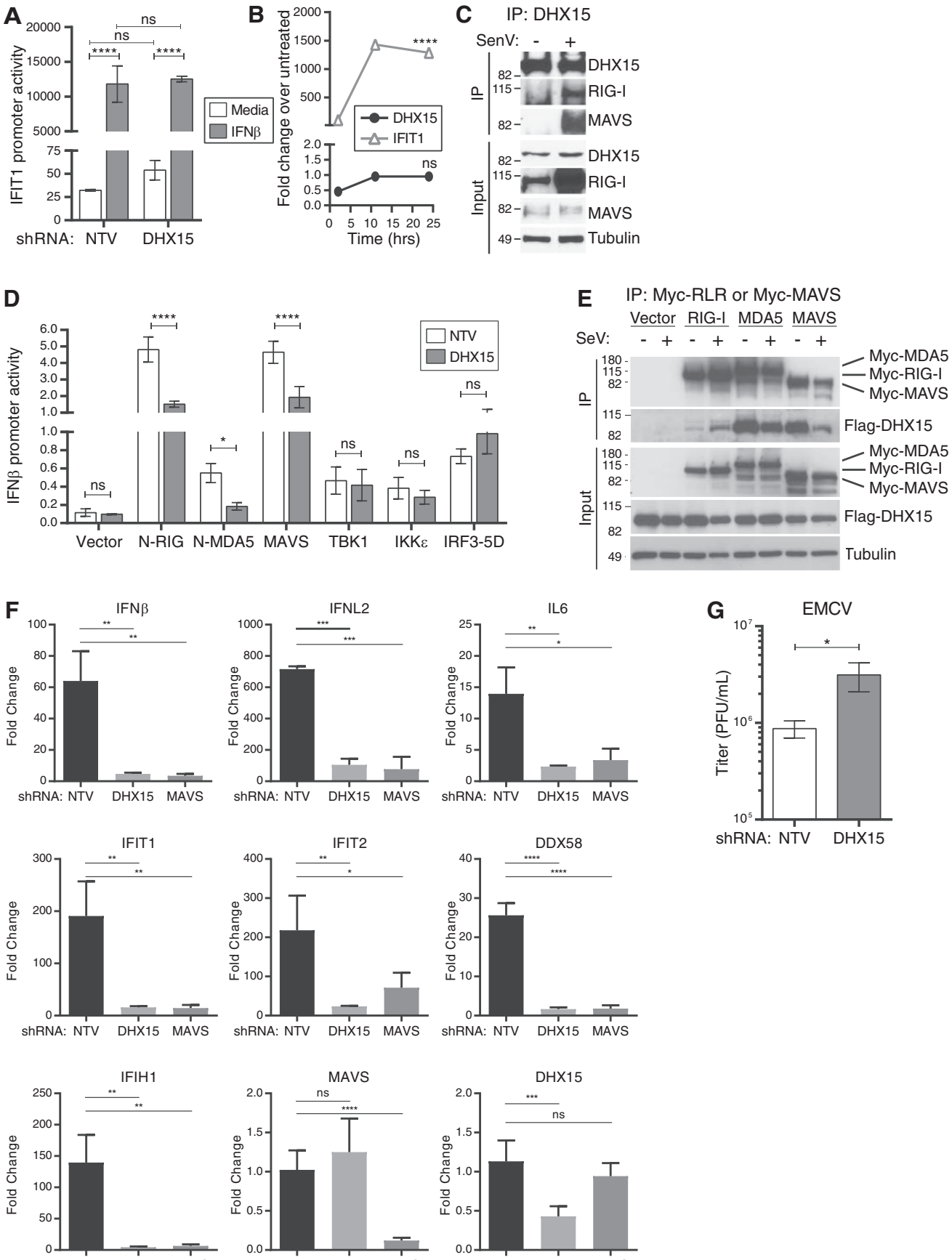
A
IFIT1 promoter activity
shRNA: NTV DHX15
Media
IFNβ
ns
****
B
Fold change over untreated
Time (hrs)
DHX15
IFIT1
C
IP: DHX15
SenV: - +
IP
Input
DHX15
RIG-I
MAVS
Tubulin
D
IFNβ promoter activity
NTV
DHX15
Vector
N-RIG
N-MDA5
MAVS
TBK1
IKKε
IRF3-5D
E
IP: Myc-RLR or Myc-MAVS
Vector
RIG-I
MDA5
MAVS
SeV: - + - + - + - +
Myc-MDA5
Myc-RIG-I
Myc-MAVS
Flag-DHX15
Tubulin
F
IFNβ
IFNL2
IL6
IFIT1
IFIT2
DDX58
IFIH1
MAVS
DHX15
Fold Change
shRNA: NTV DHX15 MAVS
G
EMCV
Titer (PFU/mL)
shRNA: NTV DHX15

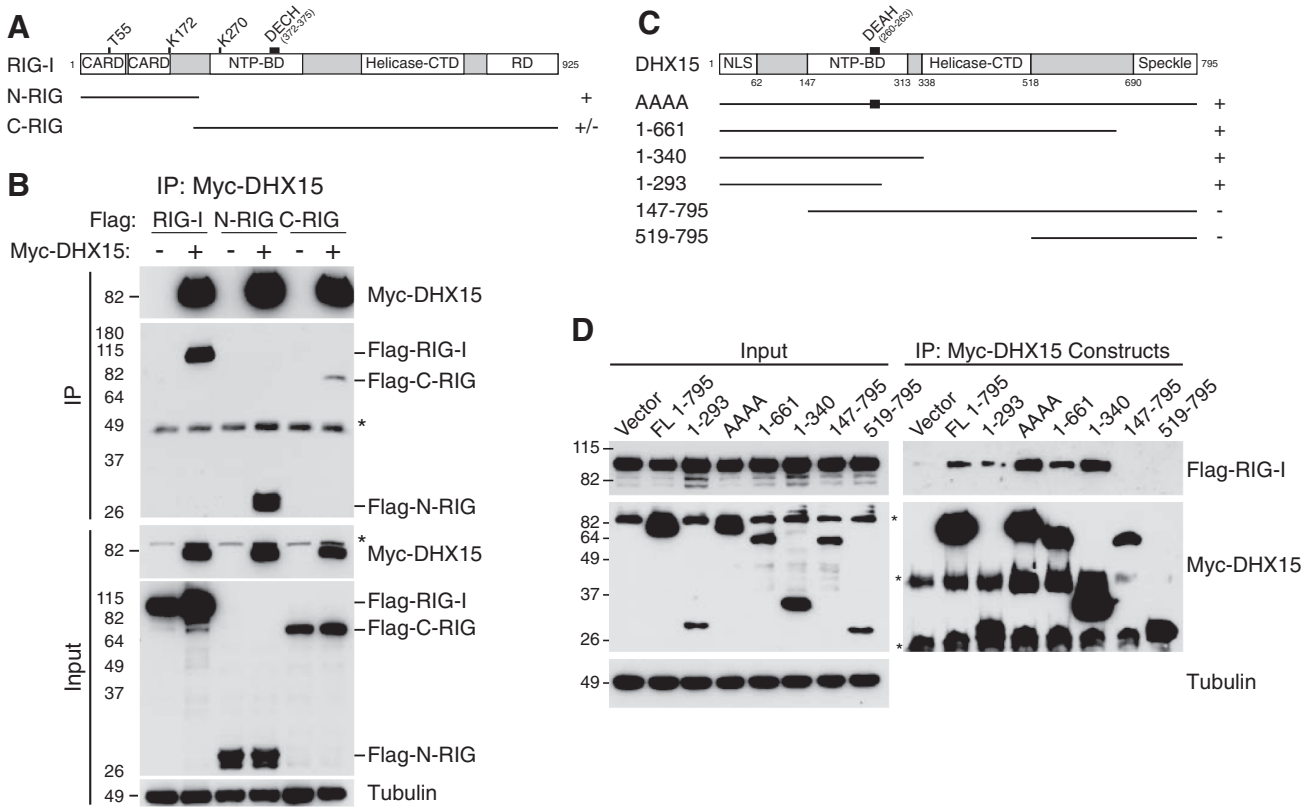

FIG. 3. N-terminus of DHX15 binds RIG-I CARDs. **(A)** Schematic of RIG-I protein and conserved motifs. Also represented are the various RIG-I truncation mutants we have created to define interactions with DHX15 by immunoprecipitation, the results of which are summarized on the *right*. **(B)** HEK293 cells were cotransfected with either a control Myc vector or a plasmid expressing Myc-DHX15 along with Flag-RIG-I constructs that express full-length RIG-I (aa 1–925), the constitutively active N-RIG (aa 1–228), or the dominant negative C-RIG (aa 219–925). Cell lysates were prepared from which Myc-DHX15 was immunoprecipitated using an anti-Myc mouse monoclonal antibody. Coprecipitating proteins were eluted from the beads in SDS-PAGE sample buffer and analyzed by Western blot analysis for various Flag-tagged RIG-I proteins. Twenty micrograms of total cell lysate was analyzed on SDS-PAGE Western blot to confirm protein expression and labeled as input. *Asterisk* denotes a nonspecific band detected by immunoblot analysis. **(C)** Schematic of DHX15 protein and conserved motifs. Also represented are the various DHX15 truncation mutants we have created to define interactions with RIG-I by immunoprecipitation, the results of which are summarized on the *right*. **(D)** HEK293 cells were cotransfected with FLAG-RIG-I along with either a control Myc vector or a plasmid expressing Myc-tagged full-length DHX15 (aa 1–795), Myc-tagged DHX15 mutants with N-terminal truncations aa 147–795 and 519–795, Myc-tagged DHX15 mutants with C-terminal truncations aa 1–661, 1–340, and 1–293, or Myc-tagged DHX15 with alanine mutations in its DEAH box (AAAA). Cell lysates were prepared from which Myc-tagged proteins were immunoprecipitated using an anti-Myc mouse monoclonal antibody. Coprecipitating proteins were eluted from the beads in SDS-PAGE sample buffer and analyzed by immunoblot analysis for Myc-DHX15 and FLAG-RIG-I. Twenty micrograms of total cell lysate was analyzed on SDS-PAGE immunoblot to confirm expression of the various constructs as input. *Asterisks* denote nonspecific bands as detected by immunoblot analysis.

construct encoding just the tandem N-terminus CARDs associates with Myc-DHX15 to levels equivalent to that of full-length RIG-I (Fig. 3B).

The DHX15 protein structure consists of domains that are typical of a DExD/H box helicase (Fig. 3C): a highly conserved DEAH sequence (aa 149–322), a helicase C-terminal domain (Helicase-CTD, aa 338–518), and a nucleotide-binding domain (NTP-BD, aa 147–313). In addition, DHX15 was characterized to contain a nuclear localization signal (aa 1–62) and a second domain important for speckle formation and nucleolar association (aa 690–795), both domains that are required for the pre-mRNA splicing activities of DHX15 (Fouraux and others 2002). We created mutant constructs truncated at both ends, and a point mutant in which the 4 residues within the DEAH motif (aa 260–263) were mutated into alanines that would interfere with ATP hydrolysis and therefore predicted to disrupt helicase and RNA-binding activities (Martin and others 2002).

The DHX15 C-terminus was not essential for binding to RIG-I nor did alanine substitution of the DEAH motif disrupt DHX15 binding to RIG-I (Fig. 3D). We found that the N-terminal 293 aa region of DHX15 consisting of the DEAH sequence was sufficient to impart binding to RIG-I. The data further suggest that the DHX15 ATPase activity is not required for this interaction. However, despite similar levels of expression as wild-type DHX15 (Fig. 1E), the overexpression of this DHX15 AAAA mutant is unable to support SeV-induced signaling to the IFN-β promoter (Fig. 1D). The data indicate that although an intact DEAH box is not essential for DHX15 to associate with RIG-I, it is required for DHX15-

facilitated innate immune signaling. Taken together, our observations indicate that the DHX15 N-terminal region mediates binding to the RIG-I CARDs.

DHX15 is an RNA PAMP-binding protein

As a DEAH RNA helicase, DHX15 is predicted to bind RNA and hydrolyze ATP toward biological activities (Wen and others 2008; Tannukit and others 2009; Niu and others 2012; Hu and others 2013; Chen and others 2014). Because of its involvement in viral RNA-sensing pathways, we conducted a comparative assessment of DHX15 binding to known PAMPs and non-PAMP RNA motifs previously defined in our studies of RIG-I (Saito and others 2008; Schnell and others 2012). We first assessed DHX15 binding to polyU/UC and xRNA, 2 5′ppp RNA segments derived from the HCV genome. The polyU/UC is a 100-nucleotide ssRNA motif that is a potent PAMP and ligand of RIG-I. The xRNA is a stem-loop structure of approximately the same length located just adjacent to polyU/UC in the 3′ untranslated region of the HCV genome. The xRNA is not recognized by RIG-I and lacks PAMP activity despite having a 5′ppp motif. For comparison, we included poly (I:C), a synthetic dsRNA of variable length that is a potent PAMP and ligand for both RIG-I and MDA5 (Yoneyama and others 2004; Sumpter and others 2005).

In filter-binding assays where we incubated 5 pmol of purified recombinant DHX15 protein with increasing amounts of biotinylated polyU/UC or xRNA, we observed biotinylated polyU/UC RNA but not xRNA binding to DHX15, causing polyU/UC to be retained on nitrocellulose membranes and its detection with an infrared dye-conjugated streptavidin (Fig. 4A). Quantitation of the infrared signal shows that polyU/UC binding to DHX15 occurs in RNA dose-dependent linear manner (Fig. 4B). We also evaluated binding of polyU/UC and xRNA to variable amounts of DHX15. We consistently observe a plateau of polyU/UC signal at around 5 pmol of DHX15, which likely is caused by a saturation of DHX15 binding onto nitrocellulose membranes (Fig. 4C). Under such conditions, we were able to detect binding to DHX15 with as little as 0.125 pmol polyU/UC, but still no binding to xRNA demonstrating the greater efficiency with which DHX15 binds to polyU/UC over xRNA.

We also assessed DHX15 binding to RNA by biotin-RNA pulldown assays. While we do not detect DHX15 binding to streptavidin beads alone, a comparison of the different RNAs shows preferential DHX15 binding to polyU/UC RNA over equimolar poly(I:C) RNA and background binding to xRNA (Fig. 4D). Taken together, the data reveal that DHX15 can bind to both ssRNA and dsRNA. The data also show DHX15 preferential binding to the PAMP RNA, polyU/UC, and poly(I:C).

With the ability to distinguish between RNA species, DHX15 could potentially function as a PRR independent of RIG-I. To test this hypothesis, we assessed whether we could genetically reconstitute innate immune signaling to a Huh7 cell line with CRISPR-directed deletion of RIG-I. As expected with SeV infection at a suboptimal dose of 20 HAU/mL, we detect no IFN-β promoter activation in the RIG-I knockout cell and only modest IFN-β promoter activation in the CRISPR control cells, in which RIG-I signaling remains intact (Fig. 4E). As expected, ectopic expression of RIG-I not only enhanced IFN-β promoter activation in the control cells, it also reconstituted signaling in the knockout cells to levels similar to the control cells. In contrast, cells with ectopic expression of DHX15 showed responses no different than cells transfected with vector control. Furthermore, cells transfected to ectopically express DHX15 and RIG-I show signaling equivalent to those expressing RIG-I alone. The data show that DHX15 cannot replace RIG-I to function independently as a PRR to signal IFN-β production in response to virus infection.

DHX15 is an ATPase and cofactor that facilitates RIG-I signaling

DExD/H box helicases share conserved nucleic acid-binding and ATP-hydrolysis activities despite broad involvement in cellular processes that involve RNA (Luo and others 2013; Fitzgerald and others 2017; Kato and others 2017; Chow and others 2018). As a viral RNA sensor, RIG-I is known to hydrolyze ATP when it engages PAMP RNA, presumably so that RIG-I can prevent unintentional recognition of self-RNA and assume the necessary conformational changes to assemble into macromolecular complexes for signaling downstream innate immune responses (Lassig and others 2015; Fitzgerald and others 2017; Devarkar and others 2018; Shah and others 2018).

To determine whether RNA binding might also influence the ATPase activity of DHX15, we assessed the level of ATP hydrolysis in direct comparison with purified RIG-I (Saito and others 2008; Jiang and others 2011). While neither DHX15 nor RIG-I exhibited spontaneous ATPase activity at low protein concentration, spontaneous ATPase activity was observed in our assays as the concentration of DHX15 was increased (Fig. 5A). In contrast, as expected of a protein that only hydrolyzes ATP in the presence of PAMP RNA, we did not detect spontaneous ATPase activity with RIG-I even with increasing protein concentrations. We thus assessed RNA-induced ATPase activity of DHX15 and RIG-I. At 5 picomol of protein, RIG-I showed ATPase activity that increased with polyU/UC concentrations but not with xRNA (Fig. 5B). In contrast, DHX15 exhibited spontaneous hydrolysis of ATP regardless of the presence of RNA. These results demonstrate that DHX15 is an RNA-binding protein that recognizes defined RNA PAMP ligands but spontaneously hydrolyzes ATP regardless of the presence of RNA.

Using a low concentration of each protein that does not impart spontaneous ATPase activity, we assessed the impact of DHX15 on RIG-I hydrolysis of ATP in the presence of RNA. Under such conditions, DHX15 exhibits minimal ATPase activity that does not change with increasing RNA concentrations (Fig. 5C). As expected of RIG-I, polyU/UC but not xRNA resulted in a modest increase in ATPase activity. With xRNA, the inclusion of both DHX15 and RIG-I in the assay resulted in ATPase activity levels equivalent to that of DHX15 alone. However, the presence of polyU/UC resulted in ATPase activity levels that exceeded that which is expected of the additive effect of both RIG-I and DHX15. A linear regression analysis comparing RIG-I, DHX15, and the 2 proteins mixed together in the presence of polyU/UC results in ATPase activity curves that have significantly different slopes, suggestive of a synergistic effect when RIG-I and DHX15 are present together (RIG-I, slope represented by $m = 0.1621 \pm 0.05281$; DHX15, $m = -0.09501 \pm 0.03666$, RIG-I +DHX15 $= 0.8929 \pm 0.06044$). A parallel analysis with

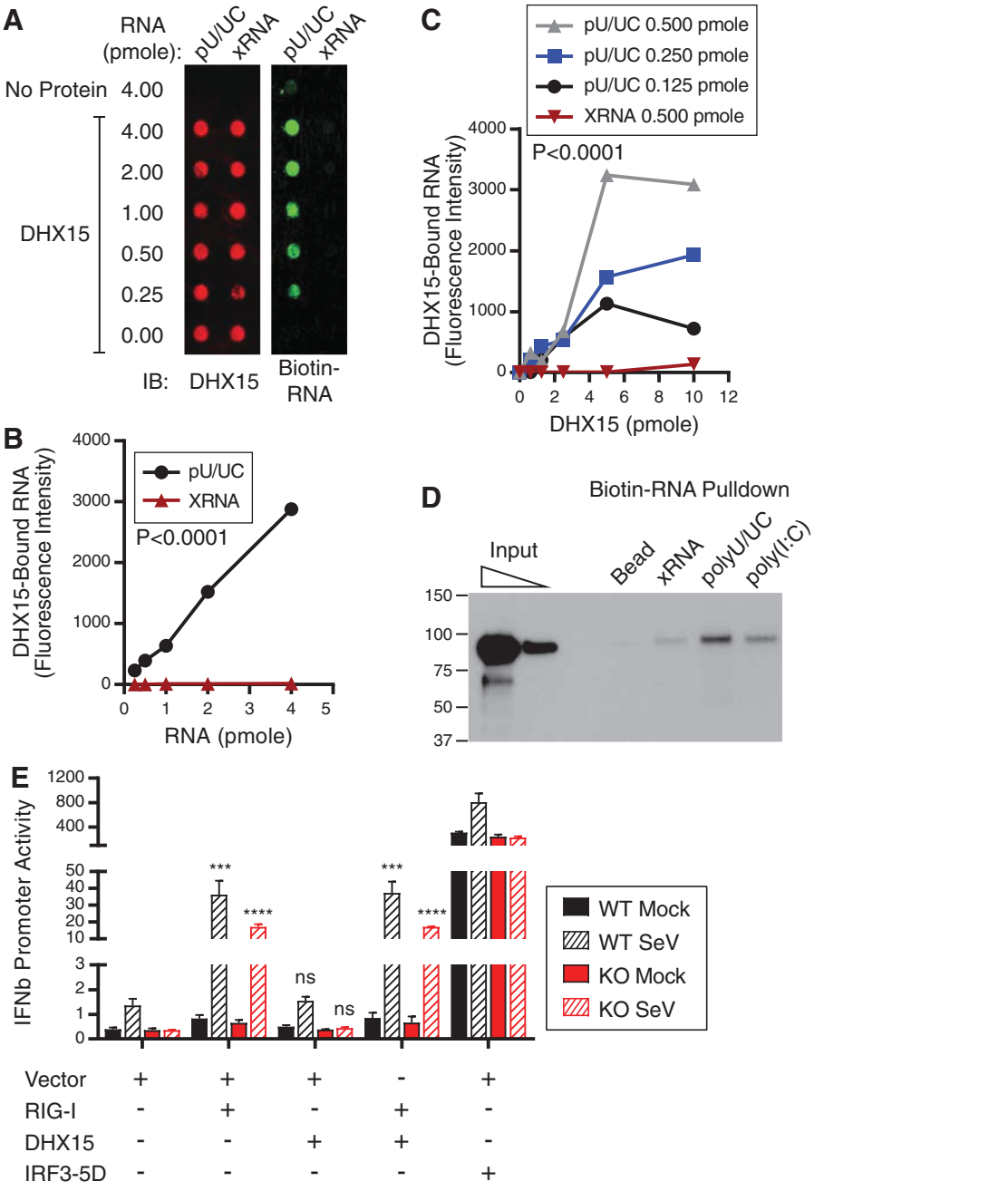

FIG. 4. DHX15 engages PAMP RNA but does not function as an independent pattern recognition receptor. **(A)** DHX15 binding to RNA was assessed by filter binding assay. A fixed concentration of purified recombinant DHX15 protein was incubated with increasing amounts of biotinylated-HCV PAMP polyU/UC or xRNA control. The mixtures were dotted onto nitrocellulose membranes and the membranes washed to remove any nonbinding RNA. No protein controls were included to reveal any nonspecific RNA binding to the nitrocellulose membranes. DHX15 protein was detected using anti-DHX15 antibody and an IRDye 680RD donkey anti-rabbit IgG (*red*). DHX15-bound RNA was retained on the membrane and detected using IRDye 800CW streptavidin (*green*). **(B)** The fluorescence intensity of DHX15-bound biotinylated RNA from independent experiments was measured and the average signal plotted as a function of RNA amount in each reaction. **(C)** Biotinylated polyU/UC RNA or xRNA binding to DHX15 across different protein concentrations with the RNA held constant at 0.125, 0.25, or 0.5 pmol in filter binding assay. **(D)** RNA binding to DHX15 was assessed by biotin-RNA pulldown assays. *In vitro* transcribed and translated DHX15 protein was incubated with streptavidin beads alone, or beads saturated for binding with biotinylated xRNA, polyU/UC, or poly(I:C) RNA. Associating DHX15 protein was eluted with SDS sample buffer and detected by immunoblot analysis. A fraction of the *in vitro* transcription and translation reaction was directly analyzed by immunoblot analysis as input. **(E)** Huh7 with CRISPR-directed RIG-I deletion or CRISPR control cells were transfected with an IFN-β promoter-driven firefly luciferase reporter plasmid, a CMV promoter-driven *Renilla* luciferase reporter plasmid, and cotransfected with either a vector control plasmid or plasmids expressing DHX15, RIG-I, or IRF3-5D. Cells were mock-infected or infected with SeV. Lysates were collected 18 h after infection and analyzed for dual luciferase reporter activity. The results are expressed as relative luciferase activity showing average ratio firefly over *Renilla*. Error bars represent standard deviations. ns, $P > 0.05$; ***$P \leq 0.001$ and ****$P \leq 0.0001$. HCV, hepatitis C virus; PAMP, pathogen-associated molecular pattern; poly(I:C), polyinosinic-polycytidylic acid.

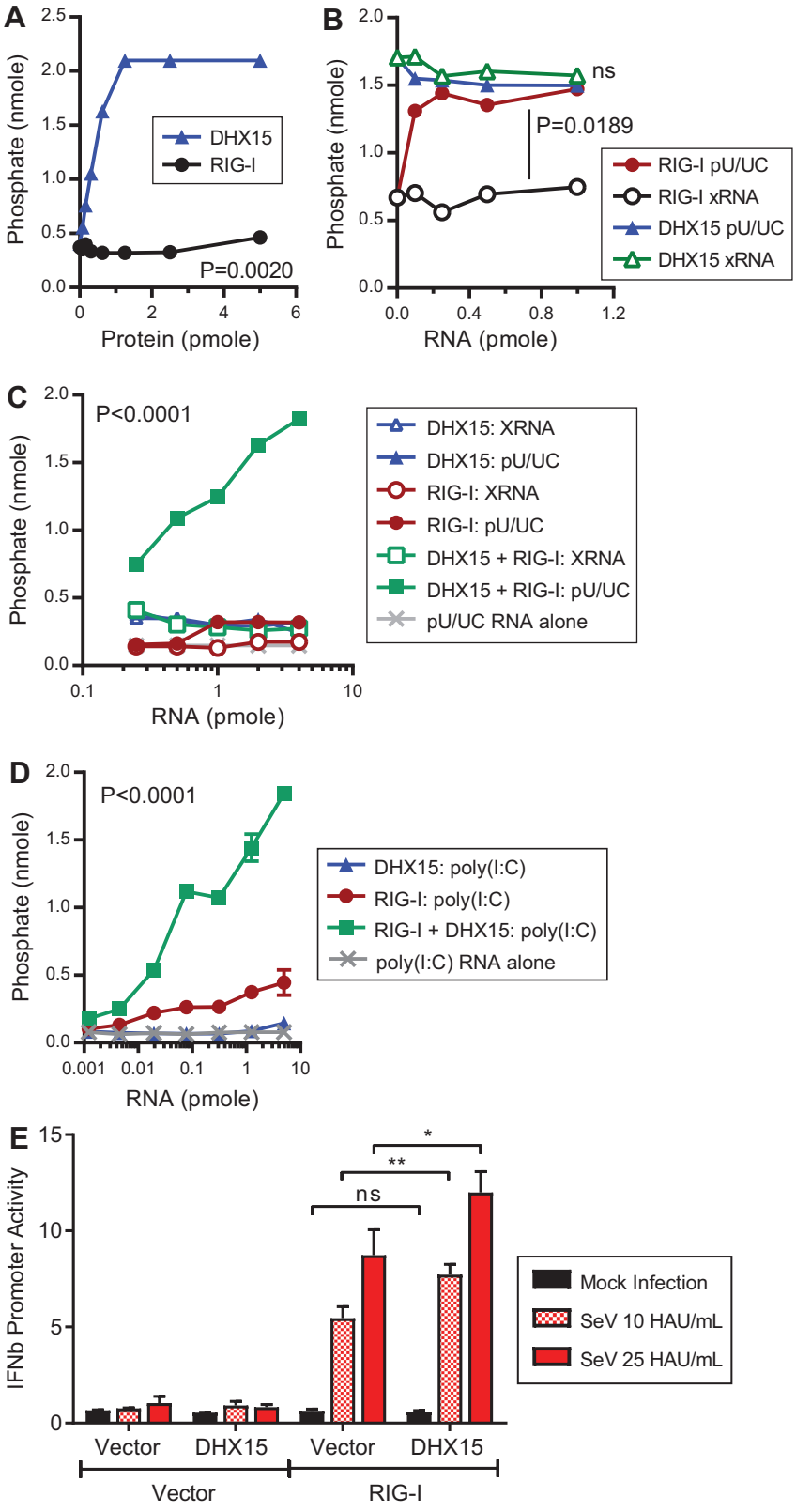

FIG. 5. DHX15 is required for optimal RIG-I PAMP RNA-dependent ATPase activity and signaling to IFN-β promoter. **(A)** Purified recombinant DHX15 and RIG-I protein were tested at various concentrations for ATP hydrolysis activity as determined by the production and release of free phosphates. Free phosphate in the reaction mix was plotted over pmol of protein used in each reaction. The slopes of the curves were compared and found to be significantly different by linear regression analysis. **(B)** Purified recombinant DHX15 or RIG-I protein was held constant in the presence of increasing polyU/UC or xRNA amounts in ATPase activity assays. Free phosphate in the reaction was plotted over pmol RNA used in each reaction. **(C)** ATPase activity was measured for DHX15 (held constant at 0.15 pmol), RIG-I (held constant at 2.5 pmol), or for both proteins in the presence of increasing amounts of xRNA or polyU/UC RNA. **(D)** ATPase activity was measured for DHX15 (held constant at 0.15 pmol), RIG-I (held constant at 2.5 pmol), or for both proteins in the presence of increasing amounts of poly(I:C) RNA. **(E)** HEK293 cells were transfected with an IFN-β promoter-driven firefly luciferase reporter plasmid, a CMV promoter-driven *Renilla* luciferase reporter plasmid, and cotransfected with either a vector control plasmid or plasmids expressing DHX15, RIG-I, or both proteins. Cells were mock-infected or infected with SeV at suboptimal innate immune stimulating levels of 10 or 25 HAU/mL. Lysates were collected 18 h after infection and analyzed for dual luciferase reporter activity. The results are expressed as relative luciferase activity showing average ratio firefly over *Renilla*. Error bars represent standard deviations. ns, $P > 0.05$; *$P \leq 0.05$; **$P \leq 0.01$. HAU, hemagglutination units.

poly(I:C) RNA also showed ATPase activity with the 2 proteins together that far exceeded that observed with either RIG-I or DHX15 alone (Fig. 5D). A linear regression analysis again showed significantly different slopes suggestive of a synergistic effect when RIG-I and DHX15 are present together (RIG-I, slope represented by m = 0.01257 ± 0.007621; DHX15, m = 0.0918 ± 0.008022, RIG-I +DHX15 = 0.4616 ± 0.04953).

Given that the DHX15 ATPase activity does not change with RNA concentrations, the data suggest that DHX15 may stimulate RIG-I hydrolysis of ATP in response to PAMP RNA, which further suggests a role for DHX15 in lowering

the threshold for RIG-I signaling activation. To test this hypothesis, we evaluated IFN-β promoter activation with ectopic DHX15 expression in the presence of limited SeV infection resulting in suboptimal RIG-I signaling activation. Ectopic DHX15 expression with RIG-I resulted in greater SeV-induced IFN-β promoter activation in HEK293 cells compared with control cells with ectopic expression of RIG-I alone (Fig. 5E), confirming that DHX15 promotes greater RIG-I signaling in response to RNA virus infection. Thus, DHX15 is an RLR-interacting protein that binds to defined RNA PAMPs and positively regulates RLR signaling that when absent, results in defective innate immune signaling leading to increased virus burden. These observations define DHX15 as a coreceptor of RLR signaling that is required for innate immune responses and the control of RNA virus infection.

Discussion

Pathogen recognition and signaling are tightly controlled processes that when aberrantly regulated result in immune dysfunction (Imaizumi and others 2007, 2008, 2010; Kitamura and others 2007; Tsugawa and others 2008). RLR signaling is regulated by the dynamic recruitment of signaling cofactors that assemble as a complex on MAVS filaments and is then licensed for signaling to initiate transcription programs that drive the innate immune response. Our results indicate that DHX15 is a component of the RLR signaling pathway through interaction with RIG-I, MDA5, and MAVS. Moreover, DHX15 can regulate MAP-kinase and NF-κB signaling that is initiated by RLR signaling (Lu and others 2014; Mosallanejad and others 2014). Importantly, our study demonstrates DHX15 to be an RLR-binding protein that regulates innate immune signaling.

DHX15 interacts with the CARDs of RIG-I and we show that on virus infection, the interaction can be further enhanced by the activation of RIG-I. Active RIG-I binds to MAVS on the MAM (Horner and others 2011; Liu and others 2012). We reveal that DHX15 interaction with RIG-I appears to be induced by RIG-I signal activation such as during RNA virus infection.

Biochemical mapping studies identified that the N-terminal region of DHX15 is responsible for mediating its interactions with RIG-I. This region of DHX15 encodes the DEAH motif that defines this protein family and has been functionally implicated in having a role in the U-12 spliceosome (Martin and others 2002; Tanaka and others 2007) as well as having a role in interacting with the human La protein (SS-B), an RNA-binding phosphoprotein that has been implicated in RNA processes, including pre-mRNA splicing, transcription, activation of the RNA-induced silencing complex (RISC), and even viral RNA replication and translation driven by internal ribosome entry sites present in viral genomes (Kim and Jang 1999; Fouraux and others 2002; Honda and others 2005; Liu and others 2011; Vashist and others 2011). This region of DHX15 might therefore function in protein interactions to support a variety of biological processes.

Curiously, a DHX15 mutant with alanine substitutions of the DEAH motif important for ATP hydrolysis and nucleotide binding retained its ability to interact with RIG-I but was unable to reconstitute SeV-induced innate immune signaling to shDHX15 knockdown cells when overexpressed, like wild-type DHX15. The data suggest that for innate immune signaling function, DHX15 requires an intact ability to hydrolyze ATP and/or bind to RNA. The data further allude to additional requirements besides physical association with RIG-I for DHX15 to facilitate RLR signaling.

In these studies, we also found DHX15 present in a complex with ectopic MDA5 and MAVS, both of which are signaling active under these overexpression conditions. Thus, DHX15 is an RLR-binding protein that can also bind to MAVS on RLR activation, possibly mediating a higher ordered complex to facilitate the RLR/MAVS interaction that drives downstream signaling. That DHX15 interacts with both RIG-I and MDA5, and its knockdown in cells was defective for innate immune gene expression in response to SeV infection and NMDA5 overexpression, and further that its knockdown in cells supported greater replication of RNA viruses known to signal through both RIG-I (SeV and VSV) and MDA5 (EMCV) points to a role for DHX15 in promoting innate immune signaling by both RLRs.

We found that purified DHX15 can bind to PAMP RNA, including the ssRNA HCV PAMP 5′ppp polyU/UC RNA and the dsRNA PAMP poly(I:C) (Saito and others 2008). However, DHX15 is not sufficient to substitute for RIG-I in innate immune responses to virus infection. We therefore propose that this RNA PAMP-binding activity and RIG-I interaction of DHX15 serve to support and enhance PAMP recognition and signaling by RIG-I. That DHX15 constitutively hydrolyzes ATP even in the absence of RNA ligands and DHX15 mutants that are defective in ATPase activity interact with RIG-I to promote signaling confirms that the ATPase activity of DHX15 is not involved in PAMP recognition and innate immune signaling (Lu and others 2014; Mosallanejad and others 2014). Importantly, the presence of DHX15 synergistically increased RIG-I ATPase activity to PAMP RNA and further enhanced RIG-I activation of the IFN-β promoter, demonstrating a role for DHX15 in facilitating RIG-I signaling activation.

Our observations are consistent with the model that DHX15 functions as a coreceptor for RLRs for PAMP RNA detection that can function by (1) sensitizing RLR detection of viral RNA, perhaps by binding to RNA and assisting in the presentation of PAMPs for RLR detection, (2) stabilizing RLR engagement of PAMP RNA for sustained signaling, and/or (3) facilitating efficient assembly of activated RLRs and MAVS into macromolecular complexes and assisting with signalosome formation to drive an innate immune response. That DHX15 is essential for RIG-I- or MDA5-dependent signaling by VSV and EMCV, respectively, suggests that rather than functioning as a specific PRR itself, it may serve as a cofactor to either RLR to facilitate signaling to MAVS. This notion is further supported by our data showing DHX15 interaction with MAVS but only under circumstances where RLR signaling is active and MAVS is in association with RIG-I and MDA5. Thus, our data support the model that once DHX15 facilitates RIG-I PAMP binding through its basal interaction through the RLR CARDs, it facilitates RIG-I interaction with MAVS to render a stable signaling complex and induction of the innate immune response.

Several helicases, including DDX60, DDX3X, DHX36, DHX29, DDX24, and DHX9, have been identified to regulate the RLR pathway (Oshiumi and others 2010; Miyashita and others 2011; Zhang and others 2011c; Ma and others 2013; Sugimoto and others 2014; Yoo and others 2014). Non-RLR helicases, DDX3X, DHX9, DDX60,

DHX33, the tripartite complex of DDX1-DDX21-DHX36, have all been identified as RNA sensors involved in non-self-RNA recognition (Oshiumi and others 2010; Miyashita and others 2011; Zhang and others 2011a, 2011c; Liu and others 2014; Shih and Lee 2014). Our study now extends this list to include DHX15 as an RLR signaling cofactor.

A key observation in our study is that DHX15 can bind specifically to both ssRNA 5′ppp HCV PAMP and to poly(I:C) dsRNA to synergistically enhance PAMP RNA-induced ATPase activity and signaling by RIG-I. Given how DHX15 is abundantly and ubiquitously expressed, we can speculate that DHX15 might facilitate PAMP RNA recognition by the RLRs, which are less abundantly expressed in the steady state until RLR expression levels increase either in response to IRF3 activation or type I IFN induction. This is also consistent with the finding that DHX15 may function as a coreceptor to NLRP6 for signaling innate immune responses in intestinal epithelial cells (Wang and others 2015). Further studies on how DHX15 can differentiate between cellular versus viral RNA will be essential in understanding its role in pathogen recognition and how it cooperates with other nucleic acid sensing pathways to initiate innate immune signaling during virus infection.

Acknowledgments

This work was supported by the National Institutes of Health grants, NIAID U19AI100625, R01AI104002, 1R01AI118916, U19AI127463, and the University of Washington/Fred Hutchinson Cancer Research Center Viral Pathogenesis Training Grant T32AI083203. We further thank Ran Dong, Alison Kell, Matthew K. Muramatsu, John Errett, and Aimee McMillan for technical assistance and Gregory Zornetzer for mass spectrometry assistance.

Author Disclosure Statement

The authors declare that there are no conflicts of interest regarding the publication of this article.

Supplementary Material

Supplementary Table S1

References

Brubaker SW, Bonham KS, Zanoni I, Kagan JC. 2015. Innate immune pattern recognition: a cell biological perspective. Annu Rev Immunol 33:257–290.

Chen YL, Capeyrou R, Humbert O, Mouffok S, Kadri YA, Lebaron S, Henras AK, Henry Y. 2014. The telomerase inhibitor Gno1p/PINX1 activates the helicase Prp43p during ribosome biogenesis. Nucleic Acids Res 42(11):7330–7345.

Chow KT, Gale M, Jr., Loo YM. 2018. RIG-I and other RNA sensors in antiviral immunity. Annu Rev Immunol 36:667–694.

Deckert J, Hartmuth K, Boehringer D, Behzadnia N, Will CL, Kastner B, Stark H, Urlaub H, Luhrmann R. 2006. Protein composition and electron microscopy structure of affinity-purified human spliceosomal B complexes isolated under physiological conditions. Mol Cell Biol 26(14):5528–5543.

Deddouche S, Goubau D, Rehwinkel J, Chakravarty P, Begum S, Maillard PV, Borg A, Matthews N, Feng Q, van Kuppeveld FJ, Reis e Sousa C. 2014. Identification of an LGP2-associated MDA5 agonist in picornavirus-infected cells. Elife 3:e01535.

Devarkar SC, Schweibenz B, Wang C, Marcotrigiano J, Patel SS. 2018. RIG-I uses an ATPase-powered translocation-throttling mechanism for kinetic proofreading of RNAs and oligomerization. Mol Cell 72(2):355.e4–368.e4.

Diamond MS, Farzan M. 2013. The broad-spectrum antiviral functions of IFIT and IFITM proteins. Nat Rev Immunol 13(1):46–57.

Errett JS, Suthar MS, McMillan A, Diamond MS, Gale M, Jr. 2013. The essential, nonredundant roles of RIG-I and MDA5 in detecting and controlling West Nile virus infection. J Virol 87(21):11416–11425.

Fitzgerald KA, McWhirter SM, Faia KL, Rowe DC, Latz E, Golenbock DT, Coyle AJ, Liao SM, Maniatis T. 2003. IK-Kepsilon and TBK1 are essential components of the IRF3 signaling pathway. Nat Immunol 4(5):491–496.

Fitzgerald ME, Rawling DC, Potapova O, Ren X, Kohlway A, Pyle AM. 2017. Selective RNA targeting and regulated signaling by RIG-I is controlled by coordination of RNA and ATP binding. Nucleic Acids Res 45(3):1442–1454.

Fouraux MA, Kolkman MJ, Van der Heijden A, De Jong AS, Van Venrooij WJ, Pruijn GJ. 2002. The human La (SS-B) autoantigen interacts with DDX15/hPrp43, a putative DEAH-box RNA helicase. RNA 8(11):1428–1443.

Foy E, Li K, Wang C, Sumpter R, Jr., Ikeda M, Lemon SM, Gale M, Jr. 2003. Regulation of interferon regulatory factor-3 by the hepatitis C virus serine protease. Science 300(5622): 1145–1148.

Gack MU. 2014. Mechanisms of RIG-I-like receptor activation and manipulation by viral pathogens. J Virol 88(10): 5213–5216.

Gack MU, Shin YC, Joo CH, Urano T, Liang C, Sun L, Takeuchi O, Akira S, Chen Z, Inoue S, Jung JU. 2007. TRIM25 RING-finger E3 ubiquitin ligase is essential for RIG-I-mediated antiviral activity. Nature 446(7138):916–920.

Honda M, Shimazaki T, Kaneko S. 2005. La protein is a potent regulator of replication of hepatitis C virus in patients with chronic hepatitis C through internal ribosomal entry site-directed translation. Gastroenterology 128(2):449–462.

Horner SM, Liu HM, Park HS, Briley J, Gale M, Jr. 2011. Mitochondrial-associated endoplasmic reticulum membranes (MAM) form innate immune synapses and are targeted by hepatitis C virus. Proc Natl Acad Sci U S A 108(35):14590–14595.

Hornung V, Ellegast J, Kim S, Brzozka K, Jung A, Kato H, Poeck H, Akira S, Conzelmann KK, Schlee M, Endres S, Hartmann G. 2006. 5′-Triphosphate RNA is the ligand for RIG-I. Science 314(5801):994–997.

Hu L, Yang F, Liu X, Xu D, Dai W. 2013. Nuclear protein IK undergoes dynamic subcellular translocation and forms unique nuclear bodies during the cell cycle. Biomark Res 1(1):11.

Imaizumi T, Arikawa T, Sato T, Uesato R, Matsumiya T, Yoshida H, Ueno M, Yamasaki S, Nakajima T, Hirashima M, Sakata K, Ishibashi Y, Toh S, Ohyama C, Satoh K. 2008. Involvement of retinoic acid-inducible gene-I in inflammation of rheumatoid fibroblast-like synoviocytes. Clin Exp Immunol 153(2):240–244.

Imaizumi T, Tanaka H, Tajima A, Tsuruga K, Oki E, Sashinami H, Matsumiya T, Yoshida H, Inoue I, Ito E. 2010. Retinoic acid-inducible gene-I (RIG-I) is induced by IFN-{gamma} in human mesangial cells in culture: possible involvement of RIG-I in the inflammation in lupus nephritis. Lupus 19(7): 830–836.

Imaizumi T, Yagihashi N, Kubota K, Yoshida H, Sakaki H, Yagihashi S, Kimura H, Satoh K. 2007. Expression of retinoic acid-inducible gene-I (RIG-I) in macrophages: possible involvement of RIG-I in atherosclerosis. J Atheroscler Thromb 14(2):51–55.

Jiang F, Ramanathan A, Miller MT, Tang GQ, Gale M, Jr., Patel SS, Marcotrigiano J. 2011. Structural basis of RNA recognition and activation by innate immune receptor RIG-I. Nature 479(7373):423–427.

Kato H, Oh SW, Fujita T. 2017. RIG-I-like receptors and type I interferonopathies. J Interferon Cytokine Res 37(5):207–213.

Kato H, Sato S, Yoneyama M, Yamamoto M, Uematsu S, Matsui K, Tsujimura T, Takeda K, Fujita T, Takeuchi O, Akira S. 2005. Cell type-specific involvement of RIG-I in antiviral response. Immunity 23(1):19–28.

Kato H, Takeuchi O, Sato S, Yoneyama M, Yamamoto M, Matsui K, Uematsu S, Jung A, Kawai T, Ishii KJ, Yamaguchi O, Otsu K, Tsujimura T, Koh CS, Reis e Sousa C, Matsuura Y, Fujita T, Akira S. 2006. Differential roles of MDA5 and RIG-I helicases in the recognition of RNA viruses. Nature 441(7089):101–105.

Kawai T, Takahashi K, Sato S, Coban C, Kumar H, Kato H, Ishii KJ, Takeuchi O, Akira S. 2005. IPS-1, an adaptor triggering RIG-I- and Mda5-mediated type I interferon induction. Nat Immunol 6(10):981–988.

Kim T, Pazhoor S, Bao M, Zhang Z, Hanabuchi S, Facchinetti V, Bover L, Plumas J, Chaperot L, Qin J, Liu YJ. 2010. Aspartate-glutamate-alanine-histidine box motif (DEAH)/RNA helicase A helicases sense microbial DNA in human plasmacytoid dendritic cells. Proc Natl Acad Sci U S A 107(34):15181–15186.

Kim YK, Jang SK. 1999. La protein is required for efficient translation driven by encephalomyocarditis virus internal ribosomal entry site. J Gen Virol 80(Pt 12):3159–3166.

Kitamura H, Matsuzaki Y, Kimura K, Nakano H, Imaizumi T, Satoh K, Hanada K. 2007. Cytokine modulation of retinoic acid-inducible gene-I (RIG-I) expression in human epidermal keratinocytes. J Dermatol Sci 45(2):127–134.

Lassig C, Matheisl S, Sparrer KM, de Oliveira Mann CC, Moldt M, Patel JR, Goldeck M, Hartmann G, Garcia-Sastre A, Hornung V, Conzelmann KK, Beckmann R, Hopfner KP. 2015. ATP hydrolysis by the viral RNA sensor RIG-I prevents unintentional recognition of self-RNA. Elife 4:e10859.

Li K, Foy E, Ferreon JC, Nakamura M, Ferreon AC, Ikeda M, Ray SC, Gale M, Jr., Lemon SM. 2005. Immune evasion by hepatitis C virus NS3/4A protease-mediated cleavage of the Toll-like receptor 3 adaptor protein TRIF. Proc Natl Acad Sci U S A 102(8):2992–2997.

Lin R, Mamane Y, Hiscott J. 1999. Structural and functional analysis of interferon regulatory factor 3: localization of the transactivation and autoinhibitory domains. Mol Cell Biol 19(4):2465–2474.

Liu HM, Loo YM, Horner SM, Zornetzer GA, Katze MG, Gale M, Jr. 2012. The mitochondrial targeting chaperone 14-3-3epsilon regulates a RIG-I translocon that mediates membrane association and innate antiviral immunity. Cell Host Microbe 11(5):528–537.

Liu Y, Lu N, Yuan B, Weng L, Wang F, Liu YJ, Zhang Z. 2014. The interaction between the helicase DHX33 and IPS-1 as a novel pathway to sense double-stranded RNA and RNA viruses in myeloid dendritic cells. Cell Mol Immunol 11(1):49–57.

Liu Y, Tan H, Tian H, Liang C, Chen S, Liu Q. 2011. Autoantigen La promotes efficient RNAi, antiviral response, and transposon silencing by facilitating multiple-turnover RISC catalysis. Mol Cell 44(3):502–508.

Loo YM, Fornek J, Crochet N, Bajwa G, Perwitasari O, Martinez-Sobrido L, Akira S, Gill MA, Garcia-Sastre A, Katze MG, Gale M, Jr. 2008. Distinct RIG-I and MDA5 signaling by RNA viruses in innate immunity. J Virol 82(1):335–345.

Loo YM, Gale M, Jr. 2011. Immune signaling by RIG-I-like receptors. Immunity 34(5):680–692.

Loo YM, Owen DM, Li K, Erickson AK, Johnson CL, Fish PM, Carney DS, Wang T, Ishida H, Yoneyama M, Fujita T, Saito T, Lee WM, Hagedorn CH, Lau DT, Weinman SA, Lemon SM, Gale M, Jr. 2006. Viral and therapeutic control of IFN-beta promoter stimulator 1 during hepatitis C virus infection. Proc Natl Acad Sci U S A 103(15):6001–6006.

Lu H, Lu N, Weng L, Yuan B, Liu YJ, Zhang Z. 2014. DHX15 senses double-stranded RNA in myeloid dendritic cells. J Immunol 193(3):1364–1372.

Luo D, Kohlway A, Pyle AM. 2013. Duplex RNA activated ATPases (DRAs): platforms for RNA sensing, signaling and processing. RNA Biol 10(1):111–120.

Ma Z, Moore R, Xu X, Barber GN. 2013. DDX24 negatively regulates cytosolic RNA-mediated innate immune signaling. PLoS Pathog 9(10):e1003721.

Martin A, Schneider S, Schwer B. 2002. Prp43 is an essential RNA-dependent ATPase required for release of lariat-intron from the spliceosome. J Biol Chem 277(20):17743–17750.

Matsumiya T, Imaizumi T, Yoshida H, Satoh K, Topham MK, Stafforini DM. 2009. The levels of retinoic acid-inducible gene I are regulated by heat shock protein 90-alpha. J Immunol 182(5):2717–2725.

Meylan E, Curran J, Hofmann K, Moradpour D, Binder M, Bartenschlager R, Tschopp J. 2005. Cardif is an adaptor protein in the RIG-I antiviral pathway and is targeted by hepatitis C virus. Nature 437(7062):1167–1172.

Michallet MC, Meylan E, Ermolaeva MA, Vazquez J, Rebsamen M, Curran J, Poeck H, Bscheider M, Hartmann G, Konig M, Kalinke U, Pasparakis M, Tschopp J. 2008. TRADD protein is an essential component of the RIG-like helicase antiviral pathway. Immunity 28(5):651–661.

Mitoma H, Hanabuchi S, Kim T, Bao M, Zhang Z, Sugimoto N, Liu YJ. 2013. The DHX33 RNA helicase senses cytosolic RNA and activates the NLRP3 inflammasome. Immunity 39(1):123–135.

Miyashita M, Oshiumi H, Matsumoto M, Seya T. 2011. DDX60, a DEXD/H box helicase, is a novel antiviral factor promoting RIG-I-like receptor-mediated signaling. Mol Cell Biol 31(18):3802–3819.

Mosallanejad K, Sekine Y, Ishikura-Kinoshita S, Kumagai K, Nagano T, Matsuzawa A, Takeda K, Naguro I, Ichijo H. 2014. The DEAH-box RNA helicase DHX15 activates NF-kappaB and MAPK signaling downstream of MAVS during antiviral responses. Sci Signal 7(323):ra40.

Niu Z, Jin W, Zhang L, Li X. 2012. Tumor suppressor RBM5 directly interacts with the DExD/H-box protein DHX15 and stimulates its helicase activity. FEBS Lett 586(7):977–983.

Oshiumi H, Sakai K, Matsumoto M, Seya T. 2010. DEAD/H BOX 3 (DDX3) helicase binds the RIG-I adaptor IPS-1 to up-regulate IFN-beta-inducing potential. Eur J Immunol 40(4):940–948.

Perkins DN, Pappin DJ, Creasy DM, Cottrell JS. 1999. Probability-based protein identification by searching sequence

databases using mass spectrometry data. Electrophoresis 20(18):3551–3567.
Saito T, Gale M, Jr. 2008. Regulation of innate immunity against hepatitis C virus infection. Hepatol Res 38(2):115–122.
Saito T, Hirai R, Loo YM, Owen D, Johnson CL, Sinha SC, Akira S, Fujita T, Gale M, Jr. 2007. Regulation of innate antiviral defenses through a shared repressor domain in RIG-I and LGP2. Proc Natl Acad Sci U S A 104(2):582–587.
Saito T, Owen DM, Jiang F, Marcotrigiano J, Gale M, Jr. 2008. Innate immunity induced by composition-dependent RIG-I recognition of hepatitis C virus RNA. Nature 454(7203):523–527.
Schnell G, Loo YM, Marcotrigiano J, Gale M, Jr. 2012. Uridine composition of the poly-U/UC tract of HCV RNA defines non-self recognition by RIG-I. PLoS Pathog 8(8):e1002839.
Seth RB, Sun L, Ea CK, Chen ZJ. 2005. Identification and characterization of MAVS, a mitochondrial antiviral signaling protein that activates NF-kappaB and IRF 3. Cell 122(5): 669–682.
Shah N, Beckham SA, Wilce JA, Wilce MCJ. 2018. Combined roles of ATP and small hairpin RNA in the activation of RIG-I revealed by solution-based analysis. Nucleic Acids Res 46(6):3169–3186.
Shih JW, Lee YH. 2014. Human DExD/H RNA helicases: emerging roles in stress survival regulation. Clin Chim Acta 436C:45–58.
Sugimoto N, Mitoma H, Kim T, Hanabuchi S, Liu YJ. 2014. Helicase proteins DHX29 and RIG-I cosense cytosolic nucleic acids in the human airway system. Proc Natl Acad Sci U S A 111(21):7747–7752.
Sumpter R, Jr., Loo YM, Foy E, Li K, Yoneyama M, Fujita T, Lemon SM, Gale M, Jr. 2005. Regulating intracellular antiviral defense and permissiveness to hepatitis C virus RNA replication through a cellular RNA helicase, RIG-I. J Virol 79(5):2689–2699.
Tanaka N, Aronova A, Schwer B. 2007. Ntr1 activates the Prp43 helicase to trigger release of lariat-intron from the spliceosome. Genes Dev 21(18):2312–2325.
Tannukit S, Crabb TL, Hertel KJ, Wen X, Jans DA, Paine ML. 2009. Identification of a novel nuclear localization signal and speckle-targeting sequence of tuftelin-interacting protein 11, a splicing factor involved in spliceosome disassembly. Biochem Biophys Res Commun 390(3):1044–1050.
Tsugawa K, Oki E, Suzuki K, Imaizumi T, Ito E, Tanaka H. 2008. Expression of mRNA for functional molecules in urinary sediment in glomerulonephritis. Pediatr Nephrol 23(3): 395–401.
Vashist S, Bhullar D, Vrati S. 2011. La protein can simultaneously bind to both 3′- and 5′-noncoding regions of Japanese encephalitis virus genome. DNA Cell Biol 30(6):339–346.
Wang P, Zhu S, Yang L, Cui S, Pan W, Jackson R, Zheng Y, Rongvaux A, Sun Q, Yang G, Gao S, Lin R, You F, Flavell R, Fikrig E. 2015. Nlrp6 regulates intestinal antiviral innate immunity. Science 350(6262):826–830.
Wen X, Tannukit S, Paine ML. 2008. TFIP11 interacts with mDEAH9, an RNA helicase involved in spliceosome disassembly. Int J Mol Sci 9(11):2105–2113.
Xu LG, Wang YY, Han KJ, Li LY, Zhai Z, Shu HB. 2005. VISA is an adapter protein required for virus-triggered IFN-beta signaling. Mol Cell 19(6):727–740.
Yoneyama M, Kikuchi M, Matsumoto K, Imaizumi T, Miyagishi M, Taira K, Foy E, Loo YM, Gale M, Jr., Akira S, Yonehara S, Kato A, Fujita T. 2005. Shared and unique functions of the DExD/H-box helicases RIG-I, MDA5, and LGP2 in antiviral innate immunity. J Immunol 175(5): 2851–2858.
Yoneyama M, Kikuchi M, Natsukawa T, Shinobu N, Imaizumi T, Miyagishi M, Taira K, Akira S, Fujita T. 2004. The RNA helicase RIG-I has an essential function in double-stranded RNA-induced innate antiviral responses. Nat Immunol 5(7): 730–737.
Yoo JS, Takahasi K, Ng CS, Ouda R, Onomoto K, Yoneyama M, Lai JC, Lattmann S, Nagamine Y, Matsui T, Iwabuchi K, Kato H, Fujita T. 2014. DHX36 enhances RIG-I signaling by facilitating PKR-mediated antiviral stress granule formation. PLoS Pathog 10(3):e1004012.
Yoshimoto R, Kataoka N, Okawa K, Ohno M. 2009. Isolation and characterization of post-splicing lariat-intron complexes. Nucleic Acids Res 37(3):891–902.
Zhang Z, Kim T, Bao M, Facchinetti V, Jung SY, Ghaffari AA, Qin J, Cheng G, Liu YJ. 2011a. DDX1, DDX21, and DHX36 helicases form a complex with the adaptor molecule TRIF to sense dsRNA in dendritic cells. Immunity 34(6):866–878.
Zhang Z, Yuan B, Bao M, Lu N, Kim T, Liu YJ. 2011b. The helicase DDX41 senses intracellular DNA mediated by the adaptor STING in dendritic cells. Nat Immunol 12(10): 959–965.
Zhang Z, Yuan B, Lu N, Facchinetti V, Liu YJ. 2011c. DHX9 pairs with IPS-1 to sense double-stranded RNA in myeloid dendritic cells. J Immunol 187(9):4501–4508.

Address correspondence to:
Dr. Yueh-Ming Loo
Department of Immunology
University of Washington
Box 358059, 750 Republican Street
Seattle, WA 98109

E-mail: looy@uw.edu

Received 6 December 2018/Accepted 1 March 2019